

Phase Behavior of Ternary Homopolymer/Diblock Blends: Microphase Unbinding in the Symmetric System

Philipp K. Janert and M. Schick*

Department of Physics, Box 351560, University of Washington, Seattle, Washington 98195-1560

Received December 26, 1996; Revised Manuscript Received April 14, 1997[⊗]

ABSTRACT: We consider the phase behavior of a symmetric AB diblock, blended with corresponding A and B homopolymers, all of equal chain length. Evaluating the phase diagram in mean-field theory at all compositions of the ternary blend, we find no hexagonal and cubic phases. However, up to three distinct lamellar phases can coexist, one being symmetric and the other two being asymmetric. For strong incompatibility, added homopolymer eventually phase separates from the microstructure. For weak segregation, the symmetric lamellar phase at moderate dilution breaks up into two coexisting lamellar phases, each asymmetrically swollen by either A or B homopolymer. These phases can be swollen indefinitely, finally unbinding into the disordered phase. As a consequence, one expects to find lamellar order at much lower diblock concentrations toward the binary sides of the phase diagram than on the isopleth.

I. Introduction

The system of symmetric AB diblock copolymer and A and B homopolymer, all of the same index of polymerization, is perhaps the simplest ternary polymer blend which undergoes microphase separation. Until recently, little attempt had been made to determine what ordered phases it displays or to map out its full phase diagram. Earlier work on this system focused on the phase coexistence of disordered phases only^{1,2} or on the interfacial activity of the diblock assembled between coexisting unstructured bulk phases.^{3–5} However, a recent Monte Carlo study⁶ obtained a cut through the full phase diagram along the isopleth, i.e. at equal concentrations of A and B homopolymer. In addition to the homogeneous phases, the diagram includes a disordered, but structured, microemulsion and a lamellar phase, but no phases possessing hexagonal or cubic symmetry. It is the point of the present paper to show that, within mean-field theory, the phase diagram has an unexpectedly rich structure. Although ordered phases of higher symmetry are unstable in mean-field theory just as in the simulations, three different lamellar phases exist, one being symmetric and two asymmetric. The symmetric one consists of roughly equidistant copolymer monolayers, separating A- and B-rich regions. For a lower overall copolymer concentration, this phase becomes unstable with respect to the formation of two coexisting phases of diblock *bilayers* in a homopolymer background. The asymmetric lamellar phases undergo complete unbinding transitions as homopolymer is added, but the symmetric one does not.

In a complete unbinding transition,^{7–9} added homopolymer swells the lamellae, and the wavelength of the lamellar phase diverges. In this limit, the system undergoes a transition to the disordered phase. At larger values of the incompatibility, measured by the Flory–Huggins parameter χ , the swelling does not increase without limit. Instead a lamellar phase of finite wavelength coexists with the disordered phase. This change of behavior with changing incompatibility can be either continuous¹⁰ or first-order.¹¹ In the latter case, a preunbinding line is expected, analogous to the prewetting line which accompanies a first-order wetting transition.¹² Matsen demonstrated¹³ within mean-field theory

that a complete unbinding occurs in the binary AB/A system at small incompatibility, while at sufficiently large incompatibility it does not. It was later shown that the transition between these regimes is first-order, and the preunbinding line, at which two lamellar phases of different wavelength coexist, was located.¹⁴

In this paper we shall see that the complete unbinding transition of the lamellar phase of AB bilayers in the majority A homopolymer remains when their cores are slightly swollen by minority B homopolymer. However when a sufficiently large concentration of the latter is added, it forms the majority component of an asymmetric lamellar phase with minority A within the cores. The two asymmetric lamellar phases coexist. Near the isopleth, a symmetric lamellar phase exists only at sufficiently large diblock concentrations. As the amount of diblock is reduced, this phase becomes unstable to the two asymmetric lamellar phases before it can unbind. Only these asymmetrically swollen lamellar phases eventually undergo complete unbinding. This result is in accord with experimental observations¹⁵ that ordered lamellar phases of bilayers in very asymmetric mixtures extend to much lower concentrations of diblock than do lamellar phases of monolayers in symmetric systems. These observations were very recently explained within the context of a phenomenological curvature model which also included the effect of the van der Waals interactions and of thermal fluctuations in the lamellar phase.¹⁶ Our microscopic calculation indicates that the relative stability of bilayer lamellar phases as compared to monolayer ones persists even when van der Waals interactions and fluctuations are negligible.

II. Phase Diagrams

A. Binary Blend. We employ the Gaussian chain model to describe the ternary mixture of symmetric AB diblock blended with A and B homopolymers. The strength of the local interaction between A and B monomers is given by the incompatibility χ . All components have the same index of polymerization. We work in the grand canonical ensemble^{17,18} and solve the mean-field equations in Fourier space.¹⁹ In addition to lamellar phases, we examine solutions of hexagonal symmetry, but do not consider hexagonally perforated lamellar or cubic structures. The phase diagram of the

[⊗] Abstract published in *Advance ACS Abstracts*, June 1, 1997.

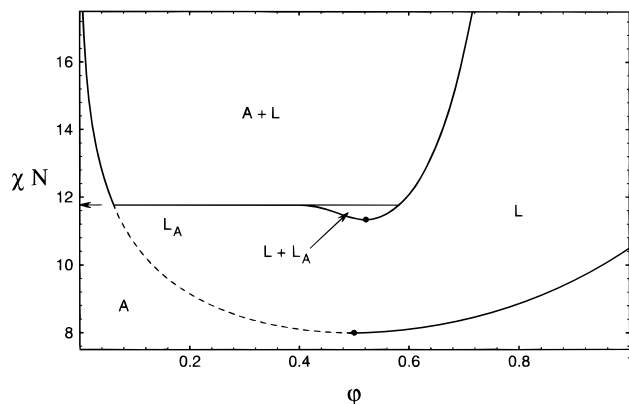


Figure 1. Calculated phase diagram for the binary homopolymer/diblock system. The incompatibility parameter χN is shown vs the copolymer volume fraction ϕ . The disordered homopolymer phase is denoted A, the dense lamellar phase L, and the swollen bilayer phase L_A . The preunbinding critical point and the Lifshitz point are shown with dots. The unbinding line is dashed, while Leibler's line of continuous transitions is shown solid. The arrow indicates the location of the first-order unbinding transition, χ_{UN} .

binary AB/A limit of the ternary system was calculated previously¹⁴ and is shown in Figure 1. At strong segregation the lamellar phase (labeled L) can only be swollen to a certain degree by additional homopolymer before phase separation occurs to an almost pure homopolymer phase (denoted A). However, for values of χN less than $\chi_{UN} = 11.766$, the lamellar phase can be swollen indefinitely. At the unbinding line, indicated by dashes in Figure 1, the separation between the lamellar sheets diverges; *i.e.* the wavenumber characterizing the lamellar phase vanishes continuously, while the Fourier coefficients of the copolymer density profile remain nonzero. The unbinding transition at χ_{UN} from bound to unbound lamellae along the lamellar/disordered phase boundary is a first-order one, with a preunbinding line which extends to a critical point at $\chi_{pu}N = 11.344$. Along the preunbinding line, two lamellar phases coexist, one of densely packed layers (L) and the other of layers strongly swollen by A homopolymer (L_A). In the strongly swollen L_A phase, copolymer rich bilayers (with the B blocks on the inside) are separated from each other by homopolymer-rich regions similar in composition to the A phase at the unbinding line.

The line of complete unbinding transitions extends to the Lifshitz critical point at $\chi_{LN} = 8.0$.¹ There it meets a line of continuous transitions from the disordered phase to a lamellar phase of nonzero wavenumber. These transitions are similar to those described by Leibler,²⁰ in that the amplitude of all Fourier coefficients of the copolymer density profile vanish continuously. (See Appendix A for a note on the nature of this transition.) Only at the Lifshitz point do both the Fourier amplitudes and the wavenumber of the lamellar phase vanish simultaneously.

B. Balanced Ternary Blend. The behavior found on the isopleth, *i.e.* for equal amounts of A and B homopolymer in the system, is shown in Figure 2. For large values of χN (*i.e.* for $\chi N \geq \chi^*N = 11.222$), the symmetric lamellar phase, L, can only be swollen to a certain extent before additional homopolymer phase separates from the microstructure. Since the homopolymers are immiscible for values of χN greater than 2.0, a three-phase region is formed at which the symmetric lamellar phase coexists with the A-rich and B-rich

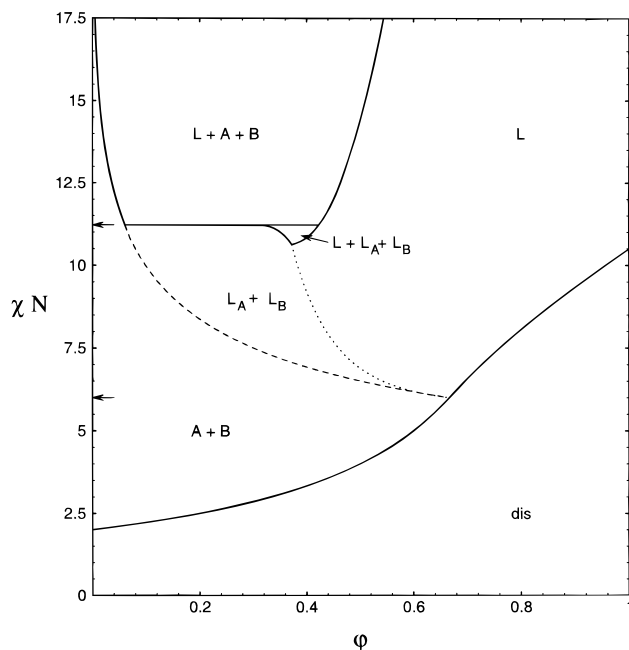


Figure 2. Calculated phase diagram for the balanced system, containing equal amount of A and B homopolymer. The notation is the same as that of Figure 1. The one-phase disordered region is denoted "dis". The consolute line of the asymmetric bilayer phases L_A and L_B , shown dotted, is schematic. The arrows indicate the locations of the unbinding transition, χ^*N and of the multicritical Lifshitz point, $\chi_M N$.

disordered phases. For values of χN less than χ^*N , there is no longer three-phase coexistence between ordered and disordered phases but rather between three ordered lamellar phases. They are the symmetric one, L, an A-rich lamellar phase L_A , and a B-rich lamellar phase L_B . In the L_A phase, thick slabs resembling the disordered A phase in composition alternate periodically with bilayers rich in B tails. At the unbinding line (denoted in Figure 2 with dashes), the spatial period of this structure diverges, and the L_A phase undergoes complete unbinding into the A-rich disordered phase. Similarly the L_B phase unbinds into the B-rich disordered phase. At copolymer concentrations less than that of three-phase coexistence but greater than that of the unbinding transition, the two asymmetric lamellar, *ordered* phases coexist, just as for lower concentrations the two asymmetric *disordered* phases coexist. The three-phase region between lamellar phases L_A , L_B , and L persists for $\chi^*N > \chi N > \chi_T N$. It ends at a tricritical point, $\chi_T N = 10.627$. For χN less than this, the two asymmetric lamellar phases merge along a line of critical points at which they form the symmetric lamellar phase. We have numerical difficulties in following this consolute line, but it is reasonable to presume that it extends to the Lifshitz multicritical point^{1,2} at $\chi_M N = 6.0$. At this point the following critical lines meet: the above-mentioned consolute line of lamellar phases; the consolute line of disordered phases; two lines of Lifshitz points which originate on the binary side¹ and which separate the sheets of Leibler transitions from the sheets of complete unbinding transitions; two lines of critical-end points at which the sheets of complete unbinding transitions intersect the first-order sheet separating A-rich and B-rich phases.

C. Full Ternary Phase Diagrams. We can now construct the full ternary phase diagrams at all values of χN . To clarify the behavior, we present a sequence

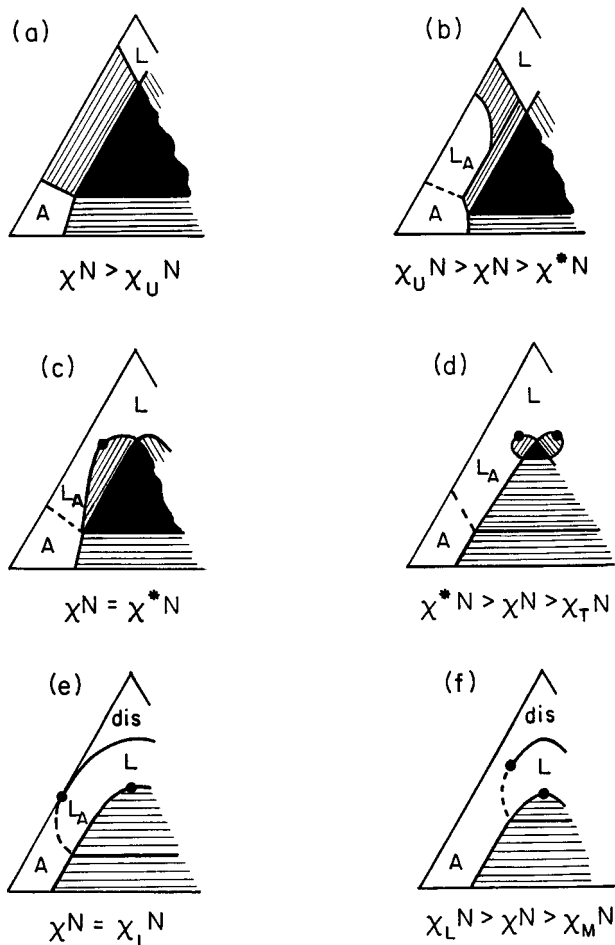


Figure 3. Schematic drawings of the left-hand side of the full ternary phase diagram for various values of χ^N . Two-phase regions are indicated by tie-lines, and three-phase triangles are shown in black.

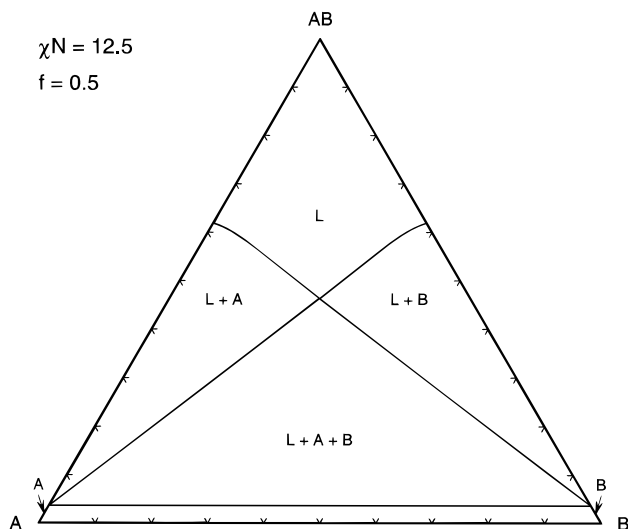


Figure 4. Calculated phase diagram for $\chi^N = 12.5$, above the unbinding transition on the binary side.

of schematic drawings (not to scale) in Figure 3, whereas the results of the numerical computation are given in Figures 4–6.

At large incompatibilities, Figure 3a and Figure 4, there are only three phases: the dense lamellar phase, and the A- and B-rich disordered phases. They can coexist. Note the very low miscibility of the pure homopolymers in Figure 4.

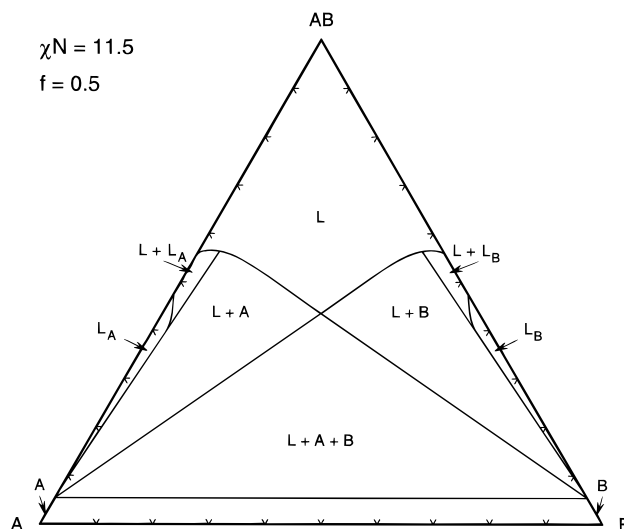


Figure 5. Calculated phase diagram for $\chi^N = 11.5$. The lamellar phase unbinds along the binary sides, but not on the isopleth.

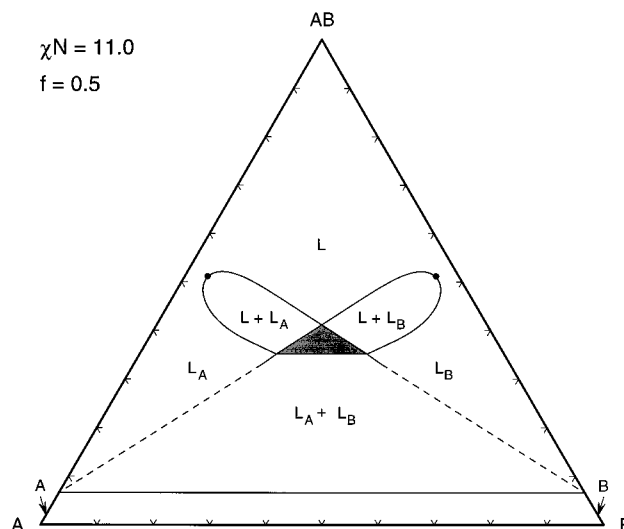


Figure 6. Calculated phase diagram for $\chi^N = 11.0$. Three-phase coexistence between the symmetric lamellar, L and two disordered phases, A and B, has been replaced by one between the symmetric lamellar and two asymmetric lamellar phases, L_A and L_B . The region of three-phase coexistence is shaded. Extrapolated phase boundaries are shown with dashes.

When χ^N is decreased to a value slightly below that of the unbinding transition on the binary side, $\chi_U^N > \chi^N > \chi_{pu}^N$, as in Figure 3b and Figure 5, the addition of B homopolymer to the binary AB/A system not only extends the unbinding transition into the interior of the three-component diagram but also extends the preunbinding region in which the symmetric lamellar phase coexists with the asymmetric A-rich lamellar phase. Note that the repeat distance of the L_A phase, coexisting with the dense L phase, increases with the amount of B homopolymer added. Three-phase coexistence is still between the symmetric lamellar and A-rich and B-rich disordered phases as long as χ^N is larger than a certain value χ^{*N} .

At this value $\chi^{*N} = 11.222$, Figure 3c, the nature of the three-phase coexistence changes. For values of χ^N less than χ^{*N} , (cf. Figure 3d and Figure 6), three-phase coexistence is between a dense lamellar phase L and two asymmetrically swollen bilayer phases (L_A and L_B). Adjacent to the three-phase triangle are two-phase regions along which different lamellar phases coexist.

The regions of $L + L_A$ and $L + L_B$ coexistence are clearly seen to be preunbinding regions. Note in particular the coexistence of two asymmetric, swollen lamellar phases, below the base of the three-phase triangle.

As χN is reduced still further, three-phase coexistence vanishes at a tricritical point at $\chi_T N = 10.629$. At smaller incompatibilities, the two asymmetric lamellar phases merge continuously at a consolute line. For values of $\chi N < 10.49$, we encounter an order/disorder transition at *high* copolymer concentration. This transition, first described by Leibler²⁰ for the pure diblock melt, appears from our numerical solutions to be continuous at all compositions. As shown in Appendix A, the Landau free energy contains no third-order invariant in the order parameter which becomes critical at the microphase transition. This is due to the fact that the copolymer is symmetric, $f = 1/2$, in the system which we examine. As there is no third-order invariant, there is no *necessity* for the transition to be first order, although it could be were the fourth-order invariant to be negative. Our numerical results indicate that this is not the case. As a result there is an entire sheet of continuous transitions separating the disordered phase from a lamellar phase of nonzero wave vector.

As the incompatibility is reduced even more, the disordered region extends further down the binary sides to lower diblock concentrations. A lamellar phase remains on the binary side and unbinds into the A-rich disordered phase at still lower compositions. At $\chi N = \chi_L N = 8.0$, Figure 3e, the lamellar phase just detaches from the binary side, and the sheet of Leibler transitions meets the sheet of complete unbinding transitions there at a Lifshitz point.¹

At still smaller values of χN , the stability region of the lamellar phase detaches completely from the binary sides, forming an island in the center of the phase diagram (Figure 3f). At the multicritical Lifshitz point, $\chi_M N = 6.0$, this island vanishes, leaving just the coexistence region of the immiscible, disordered homopolymer phases.

III. Discussion

To discuss this phase behavior, it is useful to consider the interactions between the internal interfaces in the lamellar phase. The cost of creating an interface increases with the magnitude of the density difference across it. In a lamellar phase, there is an overall attraction between neighboring layers, since the presence of the adjacent interfaces prevents the density difference across each one from attaining the value across an isolated interface. As the density difference across the interfaces increases with the degree of segregation, this attraction grows with χN . At short distances, an elastic repulsion due to the compression of the copolymers forming the layer stabilizes the lamellae at a nonzero separation.

For large values of χN , the attraction is strong enough to outweigh the entropic penalty of phase separation: It is more favorable for added homopolymer to phase separate from a dense lamellar phase than to swell it. The same mechanism prevents the formation of a symmetrically swollen phase on the isopleth for $\chi N \leq \chi^* N$: in a symmetrically swollen lamellar phase, each pair of interfaces is well separated, whereas in the bilayer phases L_A and L_B , only every second pair of interfaces is separated, while the interfaces forming each bilayer are close to each other. The binding energy gained hereby compensates the entropy loss of phase separation.

This instability of the symmetric lamellar phase to the asymmetric ones, clearly seen in Figure 6, is in good agreement with experimental observations in ternary systems containing short-chain amphiphiles.¹⁵ The major difference between our Figure 6 and experiment is that a disordered microemulsion phase is found to be stable in the region in which mean-field theory predicts a *metastable* ordered phase. The reason for this discrepancy is that our mean-field calculation ignores fluctuations which favor the disordered microemulsion phase.²¹

There are several other effects of fluctuations which will also alter the results obtained by mean-field theory. One knows that they introduce a repulsive interaction between bilayers,²² causing them to unbind more easily than in mean-field theory. However, the orientational order of the lamellae cannot be sustained when the lamellar spacing exceeds the persistence length of the bilayer,²³ with the consequence that the unbinding transition is expected to be pre-empted by a first-order transition to a disordered, but structured, sponge phase.^{24,25} It is also known that the continuous transition from the disordered phase to the lamellar phase of nonzero wavenumber is driven first-order by fluctuations.^{26,27} Finally, fluctuations can eliminate the entire coexistence region between asymmetric lamellar phases because the difference in energy between them and the symmetric lamellar phase is so small. (See Appendix B.) This is almost certainly the case in the simulation of relatively short-chain polymers.⁶ Nonetheless one expects to observe in ternary polymer blends asymmetric lamellar phases which are stable to much smaller diblock concentrations than are symmetric ones.

Acknowledgment. We are grateful to Marcus Müller for many stimulating discussions. This work was supported in part by the National Science Foundation under grant number DMR9531161.

Appendix A: Continuous Nature of the Leibler Transition

The order parameter which becomes critical at the order/disorder transition is the difference between the local density difference of A and B monomers and the average value of this difference. We let $\langle \dots \rangle$ denote thermal averages, and subscripts HA, CA, and A denote A-homopolymer, A-copolymer and total A-monomer density, respectively. Then the local order parameter is

$$\begin{aligned} \eta &= [\phi_A - \langle \phi_A \rangle] - [\phi_B - \langle \phi_B \rangle] \\ &= [(\phi_{HA} - \langle \phi_{HA} \rangle) + (\phi_{CA} - f\langle \phi_C \rangle)] - \\ &\quad [(\phi_{HB} - \langle \phi_{HB} \rangle) + (\phi_{CB} - (1-f)\langle \phi_C \rangle)] \end{aligned}$$

For $f = 1/2$, this order parameter is odd under interchange of the labels A and B, indicating the absence of any odd power of η from the Landau expansion of the free energy. Thus there is no *necessity* for the transition to be first order. This does not rule out a negative coefficient of a fourth-order invariant, which would drive the transition first-order, but our numerical results do not support such a scenario.

Appendix B: Numerical Procedure

We employ an expansion in basis functions,¹⁹ utilizing up to 40 of them, in order to solve the mean-field equations.¹⁸ We consider only ordered phases of shee-

tlike lamellae or of hexagonally-arranged cylinders. We do not find the hexagonal phase stable anywhere, although it comes close to being stable near the unbinding line. We do not consider hexagonally-perforated lamellar phases as their region of stability is probably small,¹³ and its presence would not be expected to have a major effect on the phase diagram. We also make no attempt to include form fluctuations, such as undulation or peristaltic modes. We assume the melt to be incompressible, so that there are only two independent densities (which we take to be the two homopolymer densities ϕ_A and ϕ_B), and two corresponding chemical potentials.

As pointed out elsewhere,^{14,18} calculations in the strongly swollen lamellar regime are difficult. Although the value of the free energy is slowly varying, the wavelength, and therefore the composition, depends extremely sensitively on the value of μ_A and μ_B . For example, the relative difference of fugacities, $\exp(\beta\mu)$, corresponding to the base of the three-phase triangle and to the unbinding line in Figure 6 is less than 5.0×10^{-5} . Similarly, the minimum of the free energy of strongly swollen phases is very broad and shallow as a function of the wavelength l . Thus phases with very different periods and compositions are almost equal in free energy. It was therefore impossible to calculate the phase boundaries of strongly swollen phases exactly. They are indicated in Figure 6 by dashed lines. The composition of the disordered phases does not depend strongly on the values of μ_A and μ_B , however, so that it was possible to establish the unbinding line by locating the position of the divergence of l as function of μ and then determining the composition of the corresponding disordered phase. We were not able to determine the location of the consolute line between L_A and L_B because the lamellae are very swollen close to the Lifshitz multicritical point. Therefore the density profile is far

from sinusoidal and requires an exceedingly large number of basis functions to be well represented despite the weak segregation. The consolute line curve shown dotted in Figure 2 is only schematic, being based on our best understanding of its location.

References and Notes

- (1) Broseta, D.; Fredrickson, G. H. *J. Chem. Phys.* **1990**, *93*, 2927.
- (2) Holyst, R.; Schick, M. *J. Chem. Phys.* **1992**, *96*, 7728.
- (3) Leibler, L. *Macromolecules* **1982**, *15*, 1283.
- (4) Matsen, M. W.; Schick, M. *Macromolecules* **1993**, *26*, 3878.
- (5) Werner, A.; Schmid, F.; Binder, K. *Macromolecules* **1996**, *29*, 8241.
- (6) Müller, M.; Schick, M. *J. Chem. Phys.* **1996**, *105*, 8282.
- (7) Milner, S. T.; Roux, D. *J. Phys. (Fr.) I* **1992**, *9*, 1741.
- (8) Netz, R. R.; Lipowsky, R. *Phys. Rev. Lett.* **1993**, *71*, 3596.
- (9) Lipowsky, R. *Z. Phys. B* **1995**, *97*, 193.
- (10) Leibler, S.; Lipowsky, R. *Phys. Rev. Lett.* **1987**, *58*, 1796.
- (11) Lipowsky, R. *J. Phys. (Fr.) II* **1993**, *4*, 1755.
- (12) Schick, M. In *Les Houches, Session XLVIII, 1988—Liquids at Interfaces*; J. Charvolin, Joanny, J. F., Zinn-Justin, J., Eds., Elsevier: Amsterdam, 1990.
- (13) Matsen, M. W. *Macromolecules* **1995**, *28*, 5765.
- (14) Janert, P. K.; Schick, M. *Phys. Rev.* **1996**, *E 54*, R33.
- (15) Strey, R. *Ber. Bunsen-Ges. Phys. Chem.* **1993**, *97*, 742.
- (16) Schwarz, U. S.; Swamy, K.; Gompper, G. *Europhys. Lett.* **1996**, *36*, 117.
- (17) Matsen, M. W. *Phys. Rev. Lett.* **1995**, *74*, 4225.
- (18) Janert, P. K.; Schick, M. *Macromolecules* **1997**, *30*, 137.
- (19) Matsen, M. W.; Schick, M. *Phys. Rev. Lett.* **1994**, *72*, 2660.
- (20) Leibler, L. *Macromolecules* **1980**, *13*, 1602.
- (21) Gompper, G.; Schick, M. *Self-Assembling Amphiphilic Systems*, Academic: London, 1994.
- (22) Helfrich, W. *Z. Naturforsch.* **1978**, *33A*, 305.
- (23) de Gennes, P. G.; Taupin, C. *J. Phys. Chem.* **1982**, *86*, 2294.
- (24) Golubović, L. *Phys. Rev.* **1994**, *E50*, R2419.
- (25) Morse, D. *Phys. Rev.* **1994**, *E50*, R2423.
- (26) Brazovskii, S. A. *Zh. Eksp. Teor. Fiz.* **1975**, *68*, 175; *Sov. Phys. JETP* **1975**, *41*, 85.
- (27) Fredrickson, G. H.; Helfand, E. *J. Chem. Phys.* **1987**, *87*, 697.

MA961901O